Available online at www.sciencedirect.com

ScienceDirect

Procedia CIRP 11 (2013) 328 – 333

www.elsevier.com/locate/procedia

2nd International Through-life Engineering Services Conference

Early Assessment of Defects and Damage in Jet Engines

Rafael R. Adamczuk[a]*, Joerg R. Seume[a]

[a]*Institute of 'Turbomachinery and Fluid Dynamics, Leibniz Universität Hannover, Appelstrasse 9, Hannover 30167, Germany*

* Corresponding author. Tel.: +49-511-762-17866; fax: +49-511-762-3997. *E-mail address:* adamczuk@tfd.uni-hannover.de

Abstract

The jet engine maintenance process is complex, expensive and time-consuming. It often requires engine disassembly or boroscopic examinations. In order to accelerate the process and reduce the down time of an engine we intend to develop a method to locate and characterize defects and damage at an early state, without having to disassemble the engine. The assumption is that various defects in the hot gas path of an engine have a noticeable impact on the spatial density distribution of the exhaust jet of an engine. The resulting differences in the exhaust jet pattern will be measured with the Background Oriented Schlieren method (BOS). We perform numerical simulations (CFD) in order to analyze the effects of various general defect types on the density pattern of the exhaust jet. The defects under investigation include the malfunction of one burner, the increase the turbine blade tip clearance and burned trailing edges of the blades. The changes in the pattern resulting from the defects are compared to the density distribution of the undamaged initial state. It is shown that different exhaust jet patterns can be linked to the investigated hot gas path defects. Furthermore, a BOS set-up is installed in a test cell of a helicopter engine with a two-stage axial turbine to demonstrate the applicability of the BOS method for the measurement of small density gradients resulting from temperature non-uniformities. A cold streak was inserted into the exhaust diffuser to simulate an artificial defect. The completed measurements show that the BOS method is able to detect these small variations. The present paper summarizes the results of different investigations. It presents a combination of BOS measurements of the exhaust jet and CFD simulations of defects within the hot gas path as a promising approach for evaluating the condition of a jet engine.

Selection and peer-review under responsibility of the International Scientific Committee of the "2nd International Through-life Engineering Services Conference" and the Programme Chair – Ashutosh Tiwari

Keywords: BOS; CFD; maintenance; hot gas path; jet engine

1. Introduction

The economic importance of the maintenance and regeneration of jet engines is increasing in comparison to the sale of new apparatus due to a growing fleet of aircraft. In order to reduce costs, as many components as possible should be regenerated and the total down time of each engine should be minimized. The acceleration of the process can be achieved if relevant information of damaged parts can be acquired as early as possible in order to plan the regeneration process in advance. Currently, defects and damage of engine components can be assessed either by a complete disassembly of the engine or by boroscopic examinations, both being time consuming as stated by Adamczuk *et al.* [1].

Defects within the hot gas path always have an influence on the local density and temperature of the flow. Adamczuk and Seume [2] performed CFD-simulations of the flow in a five-stage low-pressure-turbine (LPT) with large-scale temperature non-uniformities. Their results show that these local temperature variations barely mix out with the surrounding flow. In order to model malfunctions of individual burners they varied the temperature magnitude at the inlet. The worst-case defect was a complete shutdown of one burner but it was also shown that even small temperature differences have an impact on exhaust jet patterns of density and temperature. In further work, Adamczuk *et al.* [3] investigated the influence of different hot gas path defects on the density patterns at the outlet plane of a jet engine, which is summarized in this paper. The simulated defects include the complete shut-down of a burner, the loss of trailing edge material in the second rotor and stator of a two-stage high-pressure-turbine (HPT), and the increase of the clearance gap between the blade tip and the casing of the second stage rotor of the HPT. The investigations are applied to a flow geometry

Selection and peer-review under responsibility of the International Scientific Committee of the "2nd International Through-life Engineering Services Conference" and the Programme Chair – Ashutosh Tiwari

doi:10.1016/j.procir.2013.07.022

of a real aero engine. The engine consists of a combustor with 20 individual nozzles, a two-stage high-pressure turbine (HPT) and a five-stage low-pressure turbine (LPT). At the exit of the LPT eleven large exit guide vanes (EGV) are distributed over the perimeter of the outlet. The reactive flow inside a real size combustor is simulated with the method of Favre-averaged Navier-Stokes modeling. The flow through the HPT and LPT however is calculated with the method of Reynolds-averaged Navier-Stokes (RANS) modeling.

In the present study furthermore results from Adamczuk *et al.* [1] are summarized, presenting the non-intrusive Background-Oriented Schlieren (BOS) method as a quick and accurate method to measure and evaluate the three-dimensional density and temperature patterns of an exhaust jet. In order to measure three-dimensional patterns a tomographic algorithm is needed. In Adamczuk *et al.* [1], the filtered back-projection algorithm, presented and validated by Goldhahn and Seume [4] as well as Goldhahn *et al.* [5] is used. Further validation of the algorithm on a linear cascade was provided by Alhaj and Seume [6] by combining BOS with the Particle Image Velocimetry for the measurement of the total pressure loss and the kinetic energy loss coefficient. In order to demonstrate the feasibility of the approach and the possibility of measuring different temperature patterns with BOS, the method is applied to the exhaust jet of a helicopter engine.

Nomenclature

T	Temperature
n	refraction index
ρ	density
K	Gladstone-Dale-Constant
R	specific gas constant
m	distance between density field and objective
l	distance between density field and background
d	thickness of the density field
l_{px}	edge length of a pixel on the CCD chip
v_{px}	pixel shift in the image plane
f	focal length
t	line of sight
β	angle between light ray and optical axis
φ_{th}	angle between light ray and line of sight
ε	deflection angle
s	radial gap height
c	chord length

2. Simulation of defects in the hot gas path

In order to evaluate whether different hot gas path defects result in specific exhaust jet density patterns, three characteristic defects are investigated numerically in Adamczuk *et al.* [3]. As stated by Adamczuk *et al.* [1] tomographic BOS is used to evaluate time-averaged effects. Therefore only steady-state simulations are performed, which also reduces computational time and resources. As mentioned in Adamczuk *et al.* [3] for the simulation of the reactions and flow, different solvers are used. The flow and reaction inside the combustor are modeled with ANSYS Fluent. The calculations in the whole HPT were done with ANSYS CFX. Blade defects inside the HPT have been carried out with the parallel flow solver TRACE. Furthermore, the flow through the LPT is simulated with TRACE. The interfaces between the different solvers are established using two-dimensional boundary conditions, which are interpolated from the exit of the neighboring upstream component. For further details on the flow solvers, boundary conditions and numerical set-ups see Adamczuk *et al.* [3].

2.1. Modeling of combustion defects

Within this paper the modeling of three different characteristic hot gas path defects is presented. The first defect is the malfunction of one burner. The geometry of the liner and the corresponding nozzle is shown in Fig 1. In the simulation of the 90° segment with five burners it assumed that one nozzle does not provide any fuel.

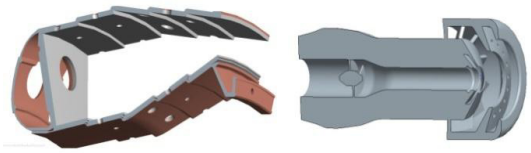

Fig. 1. (left) liner geometry; (right) nozzle geometry (Adamczuk *et al.* [3])

According to Adamczuk *et al.* [3] the resulting non-uniform flow through the HPT is shown in Fig. 2.

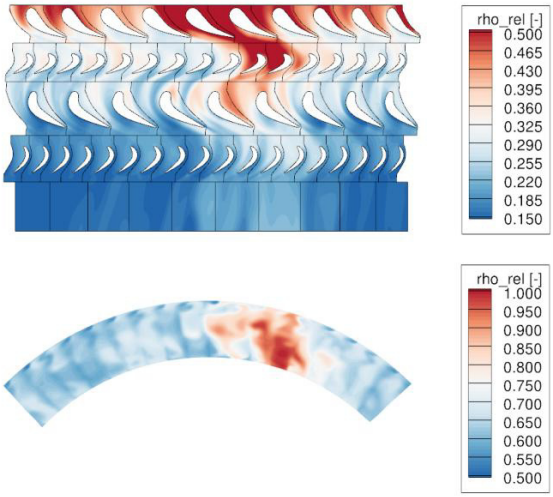

Fig. 2. Propagation of non-uniform flow from the burner malfunction through the HPT and relative density distribution at the outlet (Adamczuk *et al.* [3])

The illustration shows the relative density distribution in the outlet plane of the HPT as well as the relative density over the HPT for 50% span. For a better illustration of the results the density in the outlet plane is set relatively to the maximal value at the outlet, while the density for 50%-span is set relatively to the maximal density at the inlet of the HPT. From the illustration the progress of the non-uniformity, which results from the combustor malfunction, is clearly identifiable.

Even at the outlet of the HPT the relative density difference between the cold streak and the surrounding flow is higher than 0.3. The non-uniformity stays concentrated but affects a large area of the whole flow. A characteristical pattern can therefore be linked to a burner malfunction.

2.2. Modeling of defects with RANS

In comparison to the malfunction of one burner, defects within the HPT affect a much smaller area within in the flow. The two investigated defect types by Adamczuk *et al.* [3] are the increase of the radial gap height between the blade tip and casing and the loss of trailing edge material of the second stage rotor. The tip clearance in a rotor blade row is necessary to prevent contact between the rotating blades and the stationary casing. However, losses induced by the tip leakage flow are considerable. According to Denton [7] they account for one third of the total aerodynamic loss in a turbine stage. Bindon [8] analyzed the contributions to the tip clearance loss in a cascade configuration and determined that this loss rises linearly with increasing gap height.

Tip clearance increases during operation of the turbomachine when the blades rub on the stationary casing endwall, causing abrasion. This may occur when a hot restart is initiated during a flight envelope (Bunker [9]). In the present study, the influence of the variation of the tip clearance gap on the local density is investigated numerically. The modification of the blade is illustrated in Fig 3 (left).

Fig. 3. (left) increase of the tip clearance; (right) loss of trailing edge material Adamczuk *et al.* [3])

As a second characteristical defect in the HPT the loss of the trailing edge material is investigated. According to Meyer *et al.* [10] this defect can occur due to unintended decrease in cooling air mass flow especially during take-off. To evaluate the effect of burned trailing edges on the density of the flow, the axial chord length of the rotor blade of the second stage of the HPT is reduced, resulting in an increased trailing edge thickness. The modification of the blade is illustrated in Fig. 3 (right) showing the profiles at 0, 15, 50, 85 and 100% radial height. It is assumed that the trailing edge is burned up to the cooling holes. The variation of the edge has in general two different effects on the flow. The higher thickness results in an increase of the wake. The second effect is a change of the exit flow angle, resulting in a different incidence at the subsequent blade or vane (Adamczuk *et al.* [3]).

The effect of the two investigated defects on the power of the jet engine can already be estimated by running a throughflow code, which calculates the flow through the turbine on the meridional S2m-plane. Loss-correlations are implemented to contribute three-dimensional effects. The results where presented by Adamczuk et al. [11] and are shown in Fig. 4. The left graph illustrates the negative effect on the power for the increase in gap height, while the right graph illustrates the negative effect for the loss of trailing edge material. In both illustrations the new part and a part before the regeneration process is indicated. From the graphs it can be seen that the influence of the radial gap height is higher than the influence of the shortening of the chord. It is also clear that the monitoring of the power of an engine can provide some rudimental information about the condition of the engine. However, the loss in power or efficiency does not provide enough information to distinguish between both defects.

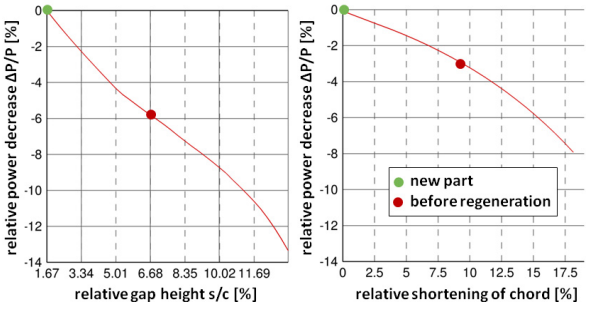

Fig. 4. Relative power decrease for (left) increased clearance gap; (right) loss of trailing edge material (Adamczuk *et al.* [11])

In Fig. 5 (left) a difference plot of the relative density distribution between the reference case and a harmed case is illustrated. The figure shows the 30° pitch at the outlet of the LPT. As mentioned before the LPT has eleven EGVs. For a better understanding of the geometry the outlet plane as well as the EGV is illustrated.

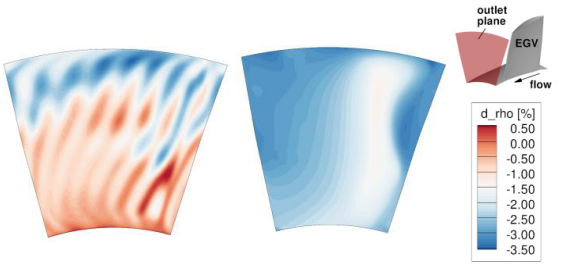

Fig. 5. Density difference to the unharmed case at the outlet of the LPT for (left) increased clearance gap; (right) loss of trailing edge material (Adamczuk *et al.* [3])

It can be observed that the relative density changes mainly in the tip region of the flow except for the area of the EGV wake, where the influence is still visible at 50% span. The maximal density decrease adds up to around -3.5%. Thus, the density variations resulting from the increased radial gap do not mix out with the complete flow but remain concentrated in the upper span regions and result in a typical change in the pattern of an exhaust jet.

The difference plot of the relative density distribution between the unharmed reference case and the burned trailing edge of the rotor blade of stage two is shown in Fig. 5 in the illustration on the right. The changes in the density distribution are not concentrated on a particular area of the outlet. The highest differences are located aside of the EGV wake adding up to -3.5%. The density within the EGV wakes is decreased by around 2%. The loss of trailing edge material, therefore leads to a clearly different pattern than the increase of the radial gap (Adamczuk *et al.* [3]). In contrast to an evaluation of the power or efficiency decrease by detecting the characteristical pattern in the exhaust jet it is likely to distinguish between both simulated defects in the HPT.

3. Exhaust jet measurements

As described by Adamczuk *et al.* [1] BOS is part of the Schlieren techniques, and sensitive to those components of the spatial derivative of the index of refraction *n* which are perpendicular to the line of sight. Along the line of sight the integral can be determined for a gas with $n \approx 1$ using Eq. 1.

$$\varepsilon \approx \tan(\varepsilon) = \sin(\varphi_{th}) \int_l \operatorname{grad}\big(n(x,y,z)\big)dt \qquad (1)$$

The angle between the direction of the refraction index gradient and the line of sight (φ_{th}) is assumed to be 90°. The Gladstone-Dale relation (Eq. 2) links the index of refraction with the density of the gas:

$$n - 1 = K \cdot \rho \qquad (2)$$

In this equation, ρ represents the density of the fluid and *K* is the Gladstone-Dale-constant. Assuming the ideal gas equation Eq. 3

$$p/\rho = R \cdot T \qquad (3)$$

a change in the temperature or pressure within the exhaust jet can be converted to a deflection of the line of sight. In the exhaust jet a constant (ambient) pressure can be assumed. A change in the temperature will therefore lead to a measurable change in the density distribution. A typical BOS set-up consists of the following main components:

- A random dot pattern on the background of the flow
- A digital camera to record the measurement images
- A computer to evaluate the measurement images

For the measurement first a picture of the background is taken without flow as a reference. Then a picture of the background is taken with flow. After a discretization into a grid of squared, overlapping windows, the images are compared using cross-correlation algorithms. A pixel shift resulting from the refraction index gradient is determined for each window. The required geometric dimensions of the BOS set-up are illustrated in Fig. 6.

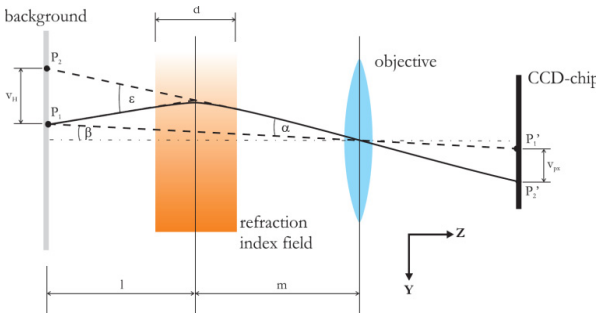

Fig. 6. BOS principle (Herbst *et al.* [12])

Based on the geometric dimensions ε can be calculated with Eq. (4).

$$\varepsilon \approx \left(1 + \frac{m}{l}\right) \cdot v_{px} \cdot l_{px} \left(\frac{l+m-f}{(l+m)\cdot f}\right) \cdot (\cos\beta)^2 \qquad (4)$$

By applying several cameras at the same time from different viewing directions during the measurement the three-dimensional density distribution in the exhaust jet can be reconstructed. Here, as already mentioned before, the filtered back-projection algorithm of Goldhahn and Seume [4] is used.

3.1. Measurement set-up

The BOS-measurements are described in detail in Adamczuk *et al.* [1], therefore in the present paper a brief summary is given. The measurements are conducted with the exhaust jet of a Turbomeca Artouste II C5 engine, a single-shaft gas turbine. The fluid is compressed in one radial impeller followed by a radial and axial diffuser. After heating of the air in an annular combustor the flow is expanded in a two-stage axial turbine. The jet flows behind the turbine through an exhaust diffuser. The output power is dissipated by an eddy current brake and the exhaust jet is ducted into an exhaust pipe. In order to simulate a non-uniformity within the temperature pattern of the exhaust jet, a pipe is mounted into the exhaust diffuser. The pipe provides a mass flow of the cold streak corresponding to 1.6% of the total mass flow of the exhaust jet. The temperature of the flow at the outlet of the piping is around 300 K. The distance between the outlet of the cooling air pipe and the first measurement plane is 31 times the diameter of the pipe while the distance to the last reconstruction plane is 39 times the diameter. The ambient pressure is measured in order to calculate the temperature distribution in the exhaust jet. For the measurements, eight cameras are used. The cameras have a 1/1.8 inch CCD chip with a resolution of 1628 x 1236 pixels. They are connected via an Ethernet switch with the measurement computer which also supplies the cameras with electrical power. The cameras are controlled and timed with a LabView code which allows for simultaneous triggering of the cameras with a frame rate of 12 frames per second during the measurements for each camera. The size of the dots on the background is chosen to correspond to four pixels on the CCD chip of the cameras.

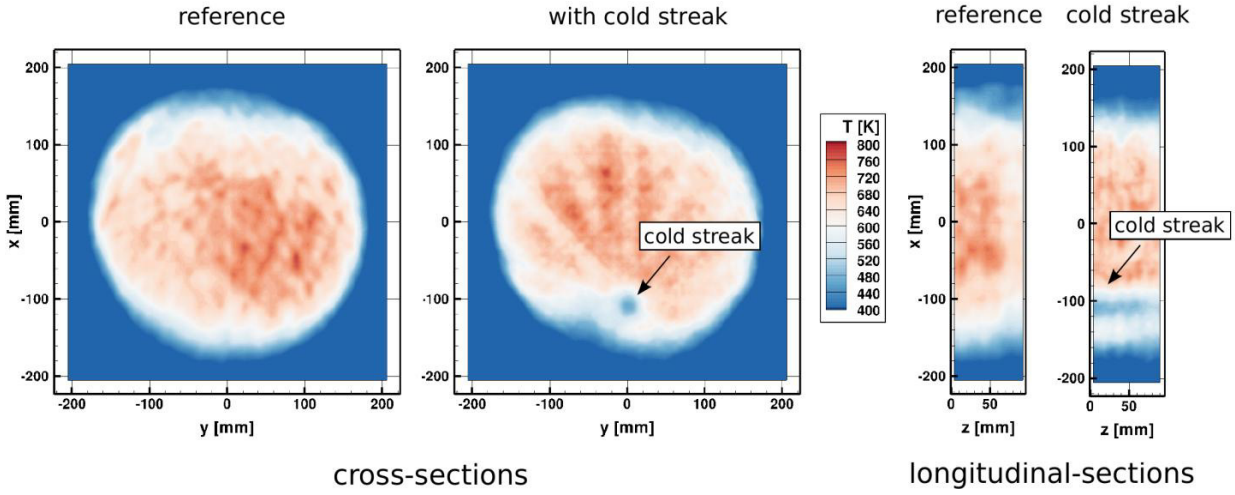

Fig. 7. Comparison of the temperature distribution in the plane perpendicular to the axis of the exhaust jet and a longitudinal plane in flow direction without (left) and with (right) cold streak (Adamczuk *et al.* [1])

During the measurements, an operating point generating 206 kW (+/- 3 kW) of shaft power is maintained. For each camera 100 images are taken. Two measurements, one without cooling flow (case 1) and one with cooling flow (case 2), are conducted. For the evaluation, of the displacement vectors between the reference and the measurement images, a window size of 16 pixels by 16 pixels is chosen and a median filter is used. The angle, the focal length of the lenses, as well as the distances between the camera, the measurement object and the background differ for each camera. So the displacement vectors have to be corrected accordingly (see Adamczuk *et al.* [1]). For that purpose, a camera, whose optical axis is perpendicular to the background, is chosen as the reference camera. The displacement vectors of all other cameras are corrected to the geometrical and optical specification of this camera.

3.2. BOS results

In Fig. 7 the temperature distribution obtained by Adamczuk *et al.* [1] is illustrated in a plane perpendicular to the jet axis for both cases - without (left) and with (right) a cold streak. The distance between the outlet of the cooling pipe and the measurement plane is around 31 times the diameter of the piping. The temperature of the exhaust jet without cooling flow is around 700-750 K. The oval shape of the exhaust jet fits the shape of the exhaust diffuser. By comparing the results with case 2, a similar shape of the jet is visible. However, a clear influence of the cold streak can be identified. The temperature of the cold streak is determined to be around 450 K. The magnitude of the temperature of the surrounding flow agrees well with case 1. Furthermore, Fig. 7 shows the temperature distribution of the longitudinal sections where the cold streak is also clearly visible. The two longitudinal sections on the far right show the progress of the exhaust jet over an axial length of 90mm. Only a small variation of the temperature and shape of the non-uniformity can be observed. As the mass flow of the cold streak is about 1.6% of the total mass flow of the exhaust jet, the results show that even temperature non-uniformities, which affect only a small part of the total mass flow barely mix out with the surrounding flow. This is visible as the cold streak still keeps concentrated only on a small area of the whole exhaust jet. Furthermore, the results clearly demonstrate that the tomographic BOS-approach can be applied for the measurement and identification of temperature non-uniformities of the temperature distribution of an exhaust jet of a gas turbine engine.

4. Conclusions and Outlook

According to Adamczuk *et al.* [1] and Adamczuk *et al.* [3] in the present study a combined approach for the evaluation of the condition of the jet engine is presented. It is intended to use the Background-Oriented Schlieren (BOS) method for measurements of the exhaust jet density distribution to evaluate non-uniformities and identify defects in the hot gas path. Within this paper the feasibility of BOS under test-cell conditions for resolving small density variations in the exhaust jet of an engine is presented. Furthermore numerical simulations are used to generate the expected density patterns in the exhaust jet of a jet engine in order to show that different defects can be attributed to characteristic exhaust jet density patterns.

In order to evaluate which density distribution patterns can be expected for various defects in the hot gas path of a jet engine, results from numerical investigations are shown in the present paper. For this purpose, three different defects, these being the failure of one combustor nozzle, the variation of the blade-tip clearance, and the shortened trailing edge of a rotor blade due to burning, are investigated. Numerical simulations of the combustor, a two-stage high-pressure turbine (HPT) and a subsequent five-stage low-pressure turbine (LPT) are performed to investigate the influence of the flow non-uniformities resulting from the different defects on the exhaust jet pattern. It is presented that the modeled defects

within the hot gas path can be attributed to a characteristic exhaust jet density pattern.

The simulations in combination with previous studies show that a shut-down of a complete nozzle has a great influence on the exhaust jet. It was presented that the low temperature region is not mixed out through the turbine and is concentrated in one area, resulting in a typical exhaust jet pattern. The increase of the clearance between a rotor blade of the second stage of the HPT results in a decrease of the density close to the casing at the outlet by up to 3.5%. The density reduction does not mix out with the whole flow of the turbine but remains concentrated near the outer casing. The influence therefore leads to a characteristic pattern. The burning of the trailing edge of the rotor blade results in an overall of the exhaust density distribution over the whole span. The relative density distribution decreases between 1.5% and 3.5%. A comparison of the influence of three different cases reveals that the defects result in completely different patterns of exhaust jet density.

For the non-intrusive measurements of the three-dimensional density and temperature patterns in the exhaust jet of a helicopter engine with a two-stage axial turbine, eight cameras are used. A cold streak was induced in the exhaust diffuser of the engine in order to experimentally demonstrate the feasibility of BOS detection of density and temperature non-uniformities in the exhaust jet. The mass flow of the cold streak was around 1.6% of the total mass flow of the jet.

Despite the small mass flow-ratio, the temperature non-uniformity does not mix out with the surrounding flow and hence a clear identification of the non-uniformity is possible. Furthermore, the temperature distribution obtained with BOS agrees with the values obtained with thermocouples within the uncertainties of each measurement technique. The results show that the tomographic BOS method can be used to measure the temperature and density distribution of an exhaust jet. Furthermore, non-uniformities can clearly be detected and identified.

In future work, BOS measurements with real defects in the hot gas path of the helicopter engine will be performed to investigate their effect on the reconstructed exhaust jet pattern. Furthermore, a methodology will be presented which will enable an investigation of the exhaust jet patterns generated with CFD simulations in respect to the delectability with BOS.

Acknowledgements

The paper presents research results of the Collaborative Research Center 871, sub projects A3, A4 and D2, which is funded by the Deutsche Forschungsgemeinschaft. The authors would like to thank Clemens Buske from the Institute of Propulsion Technology of the German Aerospace Center (DLR) for his support during the preparation of this paper.

References

[1] Adamczuk, R.; Hartmann, U.; Seume, J.: Experimental demonstration of Analyzing an Engine's Exhaust Jet with the Background-Oriented Schlieren Method, AIAA Ground Testing Conference 2013, San Diego, USA

[2] Adamczuk R.; Seume J.: Time resolved full-annulus computations of a turbine with inhomogeneous inlet conditions. International Journal of Gas Turbine, Propulsion and Power Systems, Volume 4, Number 2, June 2012

[3] Adamczuk, R.; Hennecke, C.; Dinkelacker, F., Buske, C., Röhle, I.; Seume, J.: Impacts of defects and damage in aircraft engines on the exhaust jet. In Proceedings of ASME Turbo Expo 2013: Power for Land, Sea, and Air, ASME. GT2013-95709.

[4] Goldhahn, E.; Seume, J.: The background oriented schlieren technique: sensitivity, accuracy, resolution and application to a three-dimensional density eld". Experiments in Fluids, 43(2-3), pp. 241-249.

[5] Goldhahn, E.; Alhaj, O.; Herbst, F.; Seume, J.: Quantitative measurements of three-dimensional density fields using the background oriented schlieren technique". Imaging Measurement Methods for Flow Analysis (2009), pp. 135-144.

[6] Alhaj, O.; Seume, J.: Optical investigation of profile losses in a linear turbine cascade". In Proceedings of ASME Turbo Expo 2010: Power for Land, Sea and Air, ASME. GT2010-23166.

[7] Denton, J. D.: The 1993 IGTI scholar lecture: Loss mechanisms in turbomachines.. Journal of Turbomachinery, 115(4), Oct. 1993, pp. 621–656

[8] Bindon, J. P.: The measurement and formation of tipclearance loss. Journal of Turbomachinery, 111(3), July 1989, p. 257.

[9] Bunker, R. S.: Axial turbine blade tips: Function, design, and durability. Journal of Propulsion and Power, 22(2), March 2006., pp. 271–285.

[10] Meyer, M., Parchem, R., and Davison, P.: Prediction of turbine rotor blade forcing due to in-service stator vane trailing edge damage. ASME Conference Proceedings, 2011 (54662) pp. 1193–1201.

[11] Adamczuk, R.; Hennecke, C.; Dinkelacker, F., Buske, C., Röhle, I.; Seume, J.: Assessment of Damage and Defects in Jet Engines. Conference MRO 2013, Berlin, Germany.

[12] Herbst, F., Peters, M., and Seume, J.:To the limits of the application of the bos-methods". In Proceedings of FLUCOME 2011, National Taiwan Ocean University. 065